metals

MDPI

Article

Fine Bauxite Recovery Using a Plate-Packed Flotation Column

Pengyu Zhang [1,2], Saizhen Jin [1,2], Leming Ou [1,2,*], Wencai Zhang [3,*] and Yuteng Zhu [1,2]

1 School of Minerals Processing and Bioengineering, Central South University, Changsha 410083, China; pengyu7765@csu.edu.cn (P.Z.); jinsaizhen@csu.edu.cn (S.J.); zhuyuteng@csu.edu.cn (Y.Z.)
2 Key Laboratory of Hunan Province for Clean and Efficient Utilization of Strategic Calcium-Containing Mineral Resources, Central South University, Changsha 410083, China
3 Department of Mining and Minerals Engineering, Virginia Polytechnic Institute and State University, Blacksburg, VA 24061, USA
* Correspondence: olmpaper@csu.edu.cn (L.O.); wencaizhang@vt.edu (W.Z.); Tel.: +86-0731-8883-0913 (L.O.); +540-231-6671 (W.Z.)

Received: 2 August 2020; Accepted: 24 August 2020; Published: 2 September 2020

Abstract: In this investigation, the fine-grained bauxite ore flotation was conducted in a plate-packed flotation column. This paper evaluated the effects of packing-plates on recovering fine bauxite particles and revealed the fundamental mechanisms. Bubble coalescence and break-up behaviors in the packed and unpacked flotation columns were characterized by combining Computational Fluid Dynamics (CFD) and Population Balance Model (PBM) techniques. Flotation experiments showed that packing-plates in the collection zone of a column can improve bauxite flotation performance and increase the smaller bauxite particles recovery. Using packing-plates, the recovery of Al_2O_3 increased by 2.11%, and the grade of Al_2O_3 increased by 1.85%. The fraction of −20 μm mineral particles in concentrate increased from 47.31% to 54.79%. CFD simulation results indicated that the packing-plates optimized the bubble distribution characteristics and increased the proportion of microbubbles in the flotation column, which contributed to improving the capture probability of fine bauxite particles.

Keywords: plate-packed flotation column; fine bauxite particles; bubble characteristics

1. Introduction

Most of the valuable minerals in ores are required concentration to reduce the operation costs of downstream extractive metallurgical processes. The concentration process is known as the key step of mineral processing. In the field of mineral processing, recovering fine minerals is difficult thus resulting in a lot of economic losses [1,2]. To solve these problems, column flotation technology has been developed in the past few decades [3,4]. Due to the structural features, flotation columns usually provide a higher recovery of fine minerals compared with other flotation equipment [5]. The mechanism of a traditional countercurrent flotation column is to make bubbles and mineral particles move towards each other, and then the hydrophobic particles are captured by the bubbles from the slurry, and rise with the bubbles to a froth zone. With the continuous flow of bubbles, these captured mineral particles gradually get out of the column. Consequently, the bubble size and distribution characteristics in flotation column have significant effects on the concentration performance.

After decades of progress, many different types of flotation columns have been derived and used in the industrial processing of various minerals [6–8]. Flotation columns packed with plates have specific internal structures, which impose direct effects on the flow characteristics of slurry inside the column, thereby affecting the flotation process of minerals [9–11]. For instance, a honeycomb tube

is designed as packing-plates in previous research works [12,13]. Experimental results showed that honeycomb tube can promote the generation of smaller bubbles, thereby increasing gas content, as well as particle–bubble collision probability. Moreover, the honeycomb tube packing causes turbulent rotating flow into a mild flow in the column, forming a static hydrodynamic environment and reducing the probability of detachment. The bubble behaviors was also investigated in a lab-scale cyclonic-static micro-bubble flotation column packed by sieve plates [14]. Based on Particle Image Velocimetry (PIV) and Charge-Coupled Device (CCD) camera techniques, it was found that packing non-uniform sieve plates was more effective in terms of bubble distribution equalization, air column inhabitation, and non-axial velocity decreasing.

In a previous study of fine bauxite ore column flotation [15], square packed-plates were installed in the collection zone of a flotation column in a multi-layer packing manner. Based on flotation experiments, the addition of packing-plates led to a better separation of bauxite from gangue minerals and a higher recovery of fine mineral particles. Computational Fluid Dynamics (CFD) simulation results indicated that the original intensively turbulent environment was weakened and dispersed into several units with different turbulent intensities in axial, which enhanced the separation of mineral particles with different properties. But the mechanism of improved recovery of fine mineral particles by the packing-plates has not been fully described and presented. In this present work, CFD combined with Population Balance Model (PBM) simulations were performed to characterize the bubble coalescence and break-up behaviors in the unpacked flotation column (UFC) and the plate-packed flotation column (PFC). Additionally, the effects of bubble diameter on recovering finer bauxite particles was also evaluated.

2. Materials and Methods

2.1. Flotation Apparatus and Procedures

Flotation experiments were conducted using a squared-plates column flotation apparatus (Figure 1). The flotation column has a dimension of φ80 mm × 2000 mm. This apparatus primarily consists of three subsystems: a Plexiglas flotation column, an air injection system, and a slurry circulation system. The packing-plates was made by polyethylene plates (thickness δ = 1 mm); its structure was shown in different viewpoints (see Figure 1). Three layers of packing-plates were evenly installed along the column between the slurry inlet and air inlet.

Experimental procedures of the column flotation tests were described as follows:

(1) Grind 2 kg of the bauxite ore (collected from a bauxite mine located in Henan Province, Luoyang, China) until its average particle size (D_{50}) reaches about 20 μm;
(2) Condition the feed slurry in the slurry mixing tank at room temperature and pH 9.5 (sodium carbonate as pH modifier). Add 100 g/t hexametaphosphate into the feed slurry then stir for 3 min. Followed by adding 1200 g/t sodium oleate and conditioning for 4 min. All three reagents are analytical grade supplied by Aladdin Biochem. Tech., Shanghai, China. The initial slurry solid concentration is 15%;
(3) Turn on the air compressor (0.6 MPa), and adjust air inlet flowrate to 2.5 L/min; Turn on the peristaltic pump, and adjust feed flowrate to 3.34 L/min. When foams start to flow out from the top of the column, collect the froth product as concentrate K for a period of 12 min, after which the slurry remaining in the column is collected in mixing tank as tailings X. The column flotation test is running at batch mode;
(4) Filter and dry the concentrate K and tailings X, followed by elemental analysis using X-ray fluorescence. Additionally, perform particle size analysis on the concentrate K using a laser particle size analyzer (Mastersize 2000). Both instruments are from Malver Panalytical, Malvern, UK.

Additionally, bubbles were observed in an area circled in the red box shown in Figure 1. Due to the problem of poor light transmittance during the flotation process of the bauxite ore, it was hard to

directly observe the distribution characteristics of bubbles. Therefore, bubbles were only observed in the tests without adding any mineral particles. Photos of the bubbles were captured using a Canon camera (EOS 800D, Canon, Tokyo, Japan).

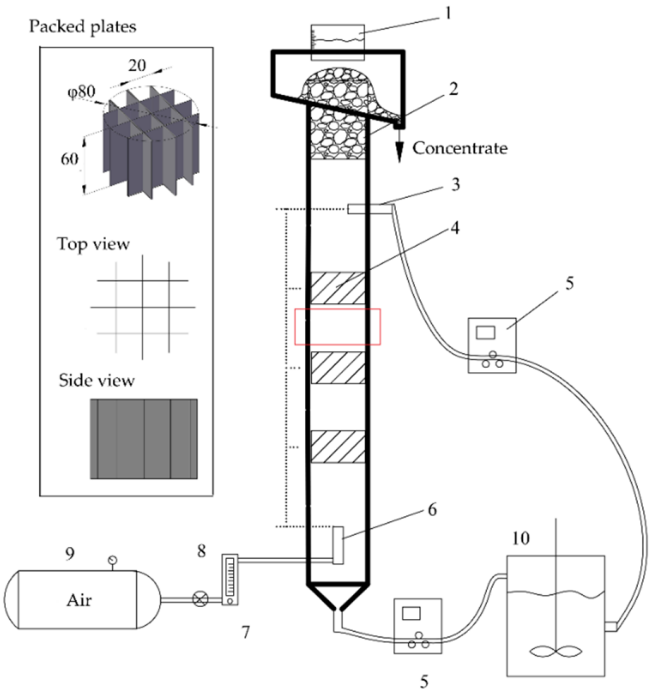

Figure 1. Experiment apparatus used for fine bauxite ore flotation: 1—Washing water device; 2—Plexiglass column; 3—Slurry inlet; 4—Packed plates; 5—Peristaltic pump; 6—Air-bubble sparger; 7—Air flowmeter; 8—Regulating valve; 9—Air compressor; 10—Slurry mixing tank.

The bauxite ore used in this research contains 44.67% of Al_2O_3 and 20.68% of SiO_2, corresponding to an aluminum oxide to silicon oxide grade (Al_2O_3/SiO_2) ratio of 2.16. Due to the relatively high content of SiO_2, the ore needs to be concentrated to improve the Al/Si ratio in order to meet the requirements on feed grade of the Bayer process. Other major components of the ore included Fe (5.19%), TiO_2 (3.76%), CaO (2.77%), K_2O (2.76%), and S (0.97%). Mica, siderite, kaolinite, anatase, quartz, calcite, and pyrite were the dominant gangue minerals.

2.2. Simulation Procedures

The simulation work was conducted in water-air two phase system using ANSYS Fluent 18.2 software (Ansys Inc., Canonsburg, PA, USA). Detailed procedures were as follows: (a) pre-processing uses ICEM for model extraction and meshing; (b) numerical calculation uses Fluent; and (c) post-processing uses CFD-post for data processing and output. This research focus on bubble characteristics affected by packing-plates in the flotation column. The collection zone of flotation column was selected as the computing domain. A geometric model of the flotation column used in the experimental apparatus was set-up as shown in Figure 2. Due to symmetry of the column in axial direction, simulation was only performed on half of the column. Additionally, boundary conditions of the calculation were based on flotation parameters. The mesh dependent tests for CFD simulation of flow calculation were conducted. The test results showed that 380,000 grids are an appropriate number to be used for UFC. Thus, a total of 380,000 grids were used for simulating flow in UFC. In case of PFC, the grid surrounding the plates was refined using the function of density box. Eulerian-Eulerian multiphase model and standard k-epsilon model were used for calculation. The bubble coalescence and break-up processes were simulated by population balance model (PBM). Parameter settings of the PBM are given in Table 1.

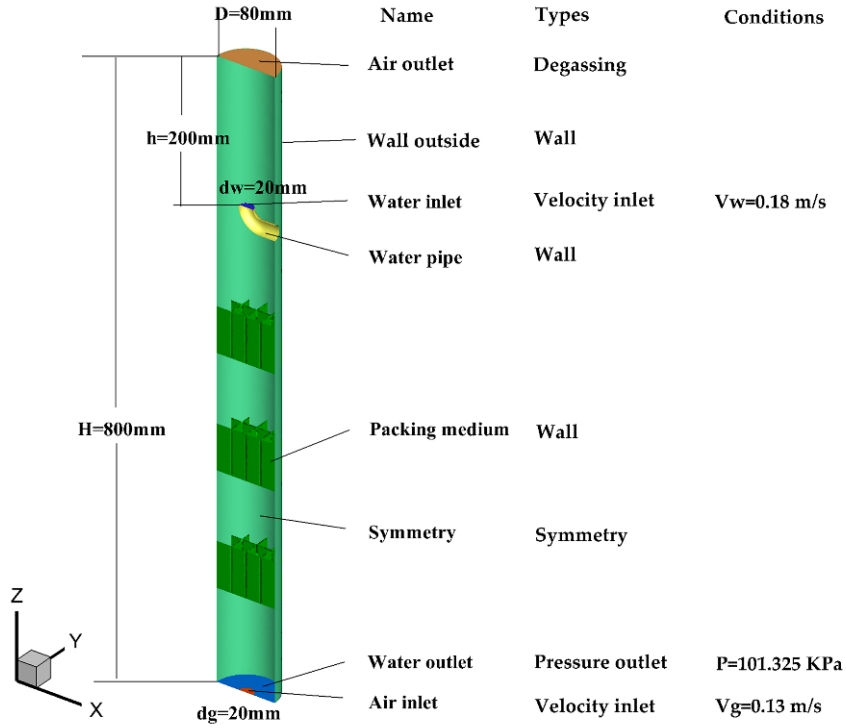

Figure 2. Geometry and boundary conditions of the flotation column for simulation.

Table 1. The parameters of population balance model (PBM).

Parameters	Value
Method	Discrete
Kv	0.52
Bubble Diameter Range	0.40~4.03 mm
Initial Bubble Diameter	1 mm
Aggregation Kernel	Luo model [16]
Breakage Kernel	Frequency-Luo model [16]; Formulation-Hagesather
Surface Tension	0.04 N/m

3. Results

3.1. Flotation Results

Flotation experiments were performed using both UFC and PFC to evaluate the effects of packing-plates on bauxite flotation performance. Figure 3 presents the flotation grade and recovery of Al_2O_3, as well as Al_2O_3/SiO_2 ratio, obtained by using UFC and PFC. It can be seen that a concentrate containing 58.4% Al_2O_3 was obtained using PFC at a recovery of 52.68%. Compared UFC, Al_2O_3 recovery and Al_2O_3 grade were increased by 2.11% and 1.85%, respectively, by using PFC. These results indicated that flotation performance of the bauxite ore was improved by packing-plates. More aluminum-enriched particles were recovered using PFC. Al_2O_3/SiO_2 ratio of the concentrated obtained using PFC reached 9.72, which is much higher than UFC. Therefore, it could be inferred that the packing-plates was able to improve the separation of aluminum minerals from silicon minerals occurring in the bauxite ore.

Particle size analysis was conducted on the concentrate obtained by using UFC and PFC. As shown in Figure 4, the fraction of −20 μm particles in UFC concentrate was 47.31 (volumetric fraction, %), however for PFC concentrate, the fraction increased up to 54.79. For particles of 20~37 μm size range, the volumetric fraction was increased by 3.06 by using PFC. Totally, the fraction of −37 μm particles in the concentrate generated from PFC increased by 10.54. Moreover, the flotation experimental results showed

that PFC concentrate had a higher Al_2O_3 grade with improved recovery (see Figure 3). Based on these findings, it can be concluded that the preferential recovery of Al_2O_3 enriched particles is attributable to the increased fraction of finer bauxite particles in the flotation concentrate. The packing-plates inside the flotation column led to improvements in the recovery of fine bauxite particles.

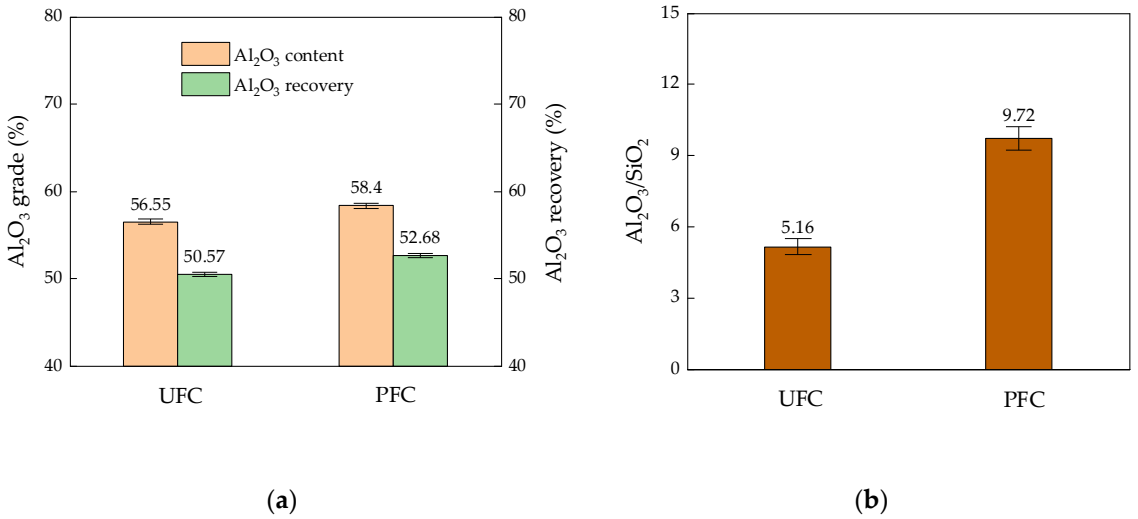

Figure 3. Flotation concentrate obtained by using unpacked flotation column (UFC) and plate-packed flotation column (PFC): (**a**) Al_2O_3 grade and recovery; (**b**) Al_2O_3/SiO_2 ratio.

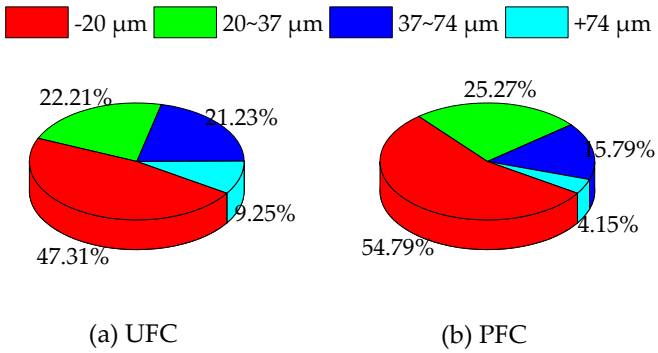

Figure 4. Particle size distribution of flotation concentrate by using (**a**) UFC and (**b**) PFC.

3.2. Bubble Characteristics

Figure 5a,b present the bubble size distribution of flows in UFC and PFC, respectively. It can be seen that bubble size increased along the axial direction and decreased along the radial direction. The bubble sizes were distributed in the range of around 0~4.2mm. When the packing-plates was used, the bubble diameter decreased in the entire flotation zone of the column. Comparing the distribution of bubbles in UFC and PFC, it can be seen that in the presence of packing-plates, bubbles in PFC have more obvious size differences, and the proportion of bubbles with smaller diameters increased. According to the simulation results, it was calculated that the mean diameter of bubbles was reduced from 3.03mm (in UFC) to 2.80mm (in PFC). The fractional distribution of bubbles in the column were also studied based on the simulation data. The results are shown in Figure 5c,d. It can be seen that the bubble diameter in UFC was primarily concentrated in the range of 2.5~4 mm. Bubbles with a diameter of 3.5 mm or larger accounted for the largest proportion, reaching 37.17%. When the column used packing-plates, the proportion of small-sized bubbles increased significantly, and the bubbles were primarily concentrated in the size range of 2.3~3.7 mm. It indicates that packing-plates could increase the proportion of microbubbles and reduce the average diameter of bubbles.

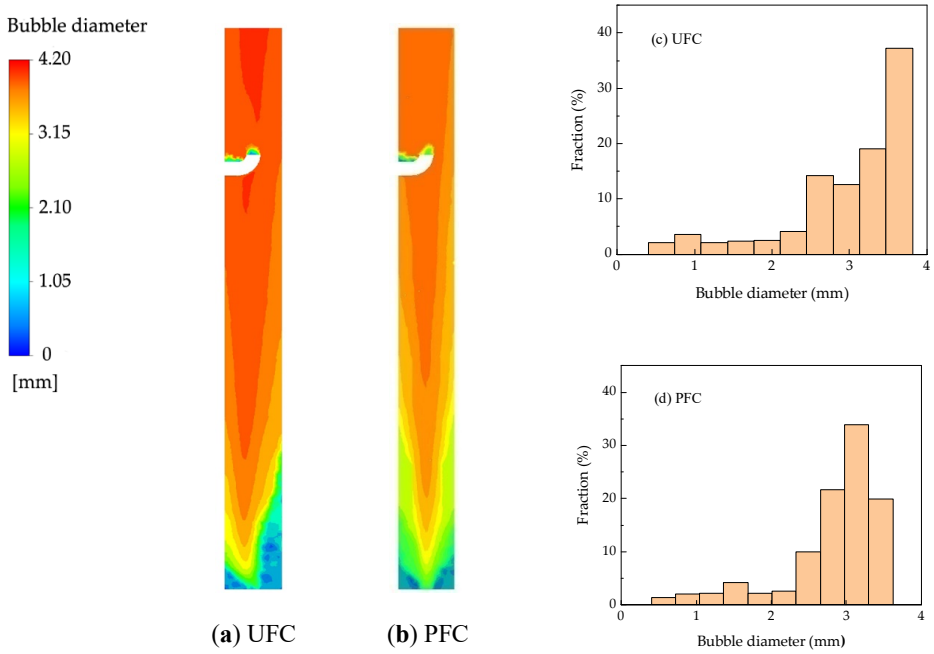

Figure 5. Bubble distribution in UFC and PFC: (**a**,**b**) Bubble size distribution in specific plane Y = 2 mm; (**c**,**d**) the fractional distribution of bubble size.

In order to verify the simulation results of bubble distribution in UFC and PFC, images of the bubbles generated in the columns under conditions similar to those used for the simulation were captured. Flows in the flotation column are three dimensional, however the images obtained using a digital camera are two dimensional. Therefore, only qualitative analysis was completed in this study. Based on the images shown in Figure 6, it can be observed that the fraction of large-size bubbles in UFC was less than PFC. Moreover, the coalescence between bubbles was reduced after packed-plates were used. This is consistent with the numerical simulation results. It is inferred that packing-plates in flotation column will inhibit bubble coalescence and promote the formation of small-size bubbles.

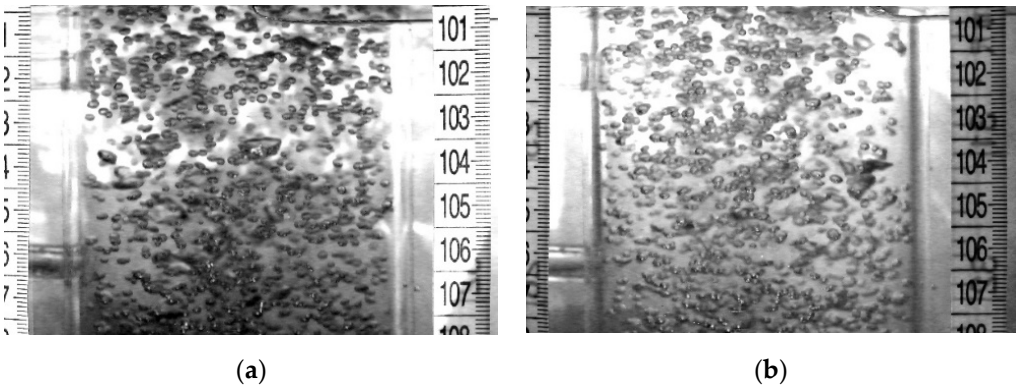

(**a**) (**b**)

Figure 6. Images of the bubbles captured in UFC and PFC: (**a**) Bubbles in UFC; (**b**) Bubbles in PFC.

3.3. Turbulence Characteristics

The movement and collision of bubbles and particles are mainly caused by fluid pulsation. In fluid mechanics, turbulent kinetic energy k is used to characterize the pulsation of large-scale vortex. The larger the value of k, the higher the pulsation velocity of large-scale vortex. Figure 7 presents the turbulent kinetic energy (TKE) distribution characteristics in UFC and PFC. It can be seen from the figure that without packing, the areas with high values of TKE were concentrated near the central axis, and decreased along both the axial and the radial direction. TKE was higher than 1×10^{-2} m^2/s^2.

After adding the packing-plates to the flotation column, the TKE inside the entire flotation column was significantly reduced. The area associated with high-value TKE was obviously reduced, and the TKE in the plates-filled area was reduced to 3.75×10^{-3} m^2/s^2. This showed that the packed plates could effectively reduce the TKE in the collection area of the flotation column, reduce the pulsating velocity of the turbulent vortex, and form a relatively mild turbulent environment.

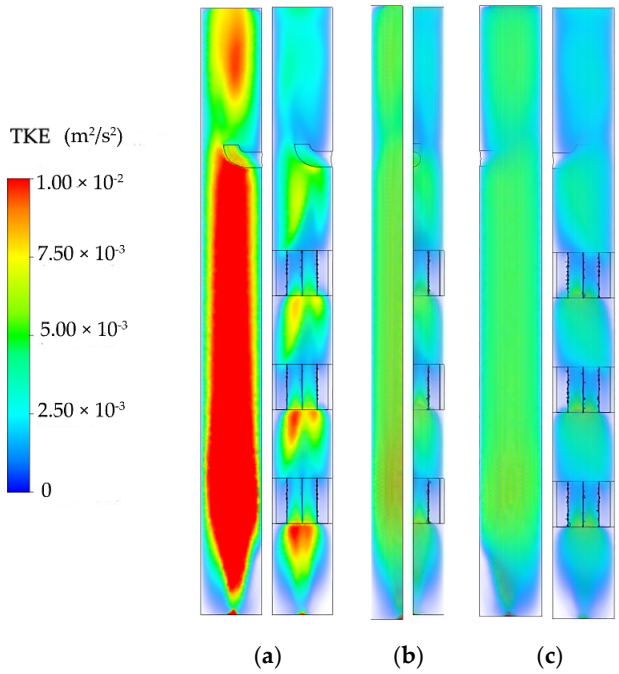

Figure 7. Turbulent kinetic energy (TKE) distribution characteristics in UFC and PFC: (**a**) Front view; (**b**) Sside view; (**c**) Rear view.

According to the simulation results, the cumulative curves of the volumetric percent of different turbulent kinetic energies are shown in Figure 8. From the results, it can be seen that the TKE in PFC was evenly distributed in the majority of the flotation column collection area. Rapid rises in the energy occurred at volume percent of 90, indicating that the volume of the area with high turbulence occupied about 10% of the collection area. In this area, the value of TKE was concentrated, the pulsating velocity of the fluid was greater, and the intensity of turbulence was greater. Compared with PFC, UFC had a higher cumulative TKE of about 0.03 m^2/s^2, which was about 3 times the value of the TKE of PFC. It showed that packing-plates in the flotation column could significantly reduce the TKE.

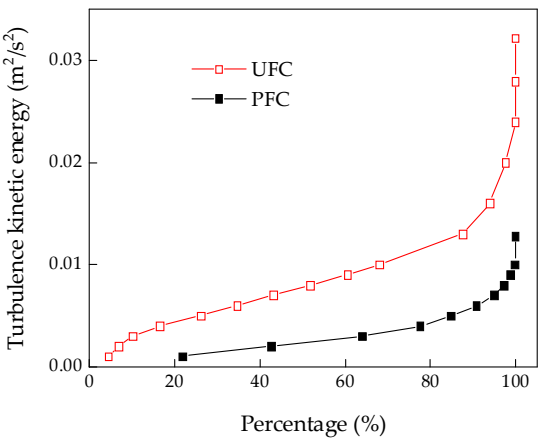

Figure 8. Turbulence kinetic energy of cumulative volume as the function of UFC and PFC.

4. Discussion

In a multiphase flow, the coalescence and break-up behaviors of bubbles are mainly affected by the surface tension of liquid phase and the hydrodynamic environment as stated by Laari and Turunen, as well as Sattar et al. [17,18]. Based on this point, a series of mathematical models about bubble coalescence and break-up have been developed by Luo and Svendsen, as well as Lehr et al. [16,19]. The main factor leading to bubble breakage is the turbulent vortex generated by the pulsation of fluid. When the turbulent vortex carries more energy than the surface energy of newly-formed bubbles, the bubble break-up may occur, and the TKE of the vortex is converted into the surface energy of the newly formed bubble. The high-energy turbulent pulsation will aggravate the collision, merging, and fragmentation behaviors of bubbles, leading to an increase in the average geometric size of the bubbles. The addition of packing-plates in the collection area of flotation column weakens the turbulent energy of flows, thus forming a milder turbulent environment (see Figure 8). Consequently, it contributes to the formation of small-size bubbles in flotation column.

According to the reports of Zhang et al. [12,13], using packed-honeycomb tubes in flotation column can increase the gas holdup of column and generate small-size bubbles. Thereby, the packed cyclonic-static micro bubble flotation column performs better in copper sulfide flotation. Xia et al. [10] performed a two-dimensional Euler–Lagrangian model to simulate the multiphase flow for some cases of baffled and packed columns. It has been found that the presence of baffles and packing will trap bubbles or hinder the upward movement of bubbles and increase the gas hold up. Combined with the simulation and test results in this study, the average diameter of the bubble group decreased after the flotation column was packed with a plates. It is easy to infer that the number of bubbles in the collection area was increased after use of packing-plates. For mineral flotation process, a higher bubble number and a smaller bubble size usually mean that the mineral particles have a higher capture rate. For fine mineral particles, the capture rate can be calculated as

$$P = P_c P_a. \tag{1}$$

The particle collision rate formula is given by Tao et al. [20]:

$$P_c = \left(\frac{3}{2} + \frac{4\mathrm{Re}_b^{0.72}}{15}\right)\left(\frac{R_p}{R_b}\right)^2. \tag{2}$$

The particle adhesion rate formula is given by Yoon and Luttrell [21]:

$$P_a = \sin^2\left\{2\arctan\exp\left[\frac{-(45 + 8\mathrm{Re}_b^{0.72})U_b t_i}{30R_b(R_b/R_p + 1)}\right]\right\}, \tag{3}$$

where Re_b is the Reynolds number of bubble, and the formula is as follows:

$$\mathrm{Re}_b = \frac{\rho_f U_b d_b}{\mu_f}. \tag{4}$$

The relative velocity of bubble is calculated using the following formula given by Schubert, as well as Shubert and Bischofberger [22,23]:

$$\sqrt{U_b^2} = 0.33\frac{\varepsilon^{4/9} d_b^{7/9}}{{\nu_f}^{1/3}}\left(\frac{\rho_b - \rho_f}{\rho_f}\right)^{2/3}. \tag{5}$$

The particle induction time formula given by Koh and Schwarz [24] is

$$t_i = \frac{75}{\theta} d_p^{0.6}. \tag{6}$$

An approximate relationship exists between the particle capture rate P_{PFC} with packing and the capture rate P_{UFC} without packing. It can be expressed as

$$P_{PFC} = CP_{UFC}, \tag{7}$$

where C is "Correlation coefficient". According to simulation results given above, the specific values are given as follows: $\mu_f = 1.003 \times 10^{-3}$ Pa·s; $\nu_f = 1.004 \times 10^{-6}$ m^2/s; $\rho_f = 998.2$ kg/m^3; $\rho_b = 1.225$ kg/m^3; and $d_p = 20$ μm; $\theta = 60°$. Turbulent dissipation rate ε and bubble diameter d_b are calculated based on the average value from the numerical simulation results. For UFC $\varepsilon_1 = 3 \times 10^{-5}$ m^2/s^3, $d_{b1} = 3.03$ mm; for PFC $\varepsilon_2 = 1 \times 10^{-5}$ m^2/s^3, $d_{b2} = 2.80$ mm. Substituting the specific values into the formula, it can be calculated $C = 1.14$. As shown in Equation (7), this means, for a mineral particle with a diameter of 20 μm, the capture probability with packing-plates is 1.14 times that of without packing.

In flotation process, reducing the size of the bubbles can not only improve the collection capacity of finer mineral particles, but also increase the volumetric concentration of bubbles in the slurry and improve the capture probability. Giving an analysis of bauxite flotation concentrate results (Figure 3) and the particle size distribution results (Figure 4), it can be seen that in PFC, the recovery of particles of smaller than 37 μm was increased by 10.54%. Among them, the proportion of particles smaller than 20 μm increased by 7.48%. The Al_2O_3 grade in the concentrate increased by 1.85%, and the recovery increased by 2.11%. These findings collectively confirmed that packing-plates inside the flotation column can increased the recovery of fine-grained mineral particles by reducing bubble diameters.

5. Conclusions

In this research, PBM incorporated with CFD techniques was performed to characterize the bubble coalescence and break-up behaviors in UFC and PFC. The effects due to application of the squared packed-plates on recovering fine bauxite particles was evaluated, and understanding of the fundamental mechanisms are achieved. The conclusions are as follows:

1. The packing-plates can significantly reduce the turbulent kinetic energy and promote the formation of a milder turbulent environment in the collection area. This will weaken the collision, merging, and fragmentation behaviors of bubbles, contributing to the formation of small-sized bubbles in flotation column.
2. Packing-plates can optimize bubble size distribution in the flotation column, and increase the proportion of micro-bubbles. According to the simulation results, the mean diameter of bubbles was reduced from 3.03 mm to 2.80 mm by packing-plates in flotation column. For mineral particles with a diameter of 20 μm, the capture probability with packing-plates is 1.14 times that of without packing.
3. Packing-plates in the collection zone of a column can improve bauxite flotation performance and enhance the recovery of fine bauxite particles. With packing, the Al_2O_3 recovery increased by 2.11%, and the Al_2O_3 grade increased by 1.85%.

Author Contributions: Conceptualization, methodology and formal analysis, P.Z.; investigation, S.J. and Y.Z.; writing—original draft preparation, P.Z.; formal analysis and writing—review and editing, W.Z.; supervision and project administration, L.O. All authors have read and agreed to the published version of the manuscript.

Funding: This work was financially supported by the National Natural Science Foundation of China (No. 51674291), and the Fundamental Research Funds for the Central Universities of Central South University (No. 2017zzts009). Key Laboratory of Hunan Province for Clean and Efficient Utilization of Strategic Calcium-containing Mineral Resources (No. 2018TP1002).

Acknowledgments: We acknowledge Beijing Lanwei Technology Co., Ltd. for providing access to ANSYS-Fluent program.

Conflicts of Interest: The authors declare no conflict of interest.

Nomenclature

φ	Diameter of column (mm)
δ	Thickness of plate(mm)
k	Turbulent kinetic energy (m^2/s^2)
P	Capture rate (%)
P_c	Collision rate (%)
P_a	Adhesion rate (%)
R_p	Particle radius (μm)
R_b	Bubble radius (mm)
Re_b	Reynolds number of bubbles
U_b	Relative velocity of bubble (m/s)
t_i	Induction time (s)
θ	Contact angle of mineral (°)
ε	Turbulent energy dissipation rate (m^2/s^3)
ρ_f	Fluid density (Kg/m^3)
μ_f	Dynamic viscosity of fluid (Pa·s)
ν_f	Kinematic viscosity of fluid (m^2/s)
d_b	Bubble diameter (mm)
ρ_b	Bubble density (Kg/m^3)
P_{PFC}	Capture rate of PFC
P_{UFC}	Capture rate of UFC

References

1. Miettinen, T.; Ralston, J.C.; Fornasiero, D. The limits of fine particle flotation. *Miner. Eng.* **2010**, *23*, 420–437. [CrossRef]
2. Santana, R.C.; Duarte, C.R.; Ataíde, C.H.; Barrozo, M.A.S. Flotation selectivity of phosphate ore: Effects of particle size and reagent concentration. *Sep. Sci. Technol.* **2011**, *46*, 1511–1518. [CrossRef]
3. Harbort, G.; Clarke, D. Fluctuations in the popularity and usage of flotation columns—An overview. *Miner. Eng.* **2017**, *100*, 17–30. [CrossRef]
4. Prakash, R.; Majumder, S.K.; Singh, A. Flotation technique: Its mechanisms and design parameters. *Chem. Eng. Process. Process Intensif.* **2018**, *127*, 249–270. [CrossRef]
5. Yianatos, J.B. Fluid flow and kinetic modelling in flotation related processes: Columns and mechanically agitated cells—A review. *Chem. Eng. Res. Des.* **2007**, *85*, 1591–1603. [CrossRef]
6. Cheng, G.; Cao, Y.; Zhang, C.; Jiang, Z.; Yu, Y.; Mohanty, M.K. Application of novel flotation systems to fine coal cleaning. *Int. J. Coal Prep. Util.* **2020**, *40*, 24–36. [CrossRef]
7. Moys, M.; Engelbrecht, J. Simulation of the behaviour of flexible baffles in flotation columns. *Chem. Eng. J. Biochem. Eng. J.* **1995**, *59*, 33–38. [CrossRef]
8. Vashisth, S.; Bennington, C.P.; Grace, J.R.; Kerekes, R.J. Column flotation deinking: State-of-the-art and opportunities. *Resour. Conserv. Recycl.* **2011**, *55*, 1154–1177. [CrossRef]
9. Ding, Y.; Wu, Y.; Li, D.; Zheng, J. Technical note a study on the mixing characteristics of a packed flotation column. *Miner. Eng.* **2001**, *14*, 1101–1105. [CrossRef]
10. Xia, Y.; Peng, F.; Wolfe, E. CFD simulation of alleviation of fluid back mixing by baffles in bubble column. *Miner. Eng.* **2006**, *19*, 925–937. [CrossRef]
11. Farzanegan, A.; Khorasanizadeh, N.; Sheikhzadeh, G.A.; Khorasanizadeh, H. Laboratory and CFD investigations of the two-phase flow behavior in flotation columns equipped with vertical baffle. *Int. J. Miner. Process.* **2017**, *166*, 79–88. [CrossRef]
12. Zhang, M.; Li, T.; Wang, G. A CFD study of the flow characteristics in a packed flotation column: Implications for flotation recovery improvement. *Int. J. Miner. Process.* **2017**, *159*, 60–68. [CrossRef]
13. Zhang, M.; Li, T.; Ma, S.; Wang, G. An experimental study of copper sulfide flotation in a packed cyclonic–static microbubble flotation column. *Sep. Sci. Technol.* **2018**, *53*, 2238–2248. [CrossRef]
14. Yan, X.; Shi, R.; Xu, Y.; Wang, A.; Liu, Y.; Wang, L.; Cao, Y. Bubble behaviors in a lab-scale cyclonic-static micro-bubble flotation column. *Asia-Pacific J. Chem. Eng.* **2016**, *11*, 939–948. [CrossRef]

15. Zhang, P.; Zhang, W.; Ou, L.; Zhu, Y.; Zhu, Z. Enhanced bauxite recovery using a flotation column packed with multilayers of medium. *Minerals* **2020**, *10*, 594. [CrossRef]
16. Luo, H.; Svendsen, H.F. Theoretical model for drop and bubble breakup in turbulent dispersions. *AIChE J.* **1996**, *42*, 1225–1233. [CrossRef]
17. Laari, A.; Turunen, I. Experimental determination of bubble coalescence and break-up rates in a bubble column reactor. *Can. J. Chem. Eng.* **2003**, *81*, 395–401. [CrossRef]
18. Sattar, M.; Naser, J.; Brooks, G. Numerical simulation of two-phase flow with bubble break-up and coalescence coupled with population balance modeling. *Chem. Eng. Process.* **2013**, *70*, 66–76. [CrossRef]
19. Lehr, F.; Millies, M.; Mewes, D. Bubble-size distributions and flow fields in bubble columns. *AIChE J.* **2002**, *48*, 2426–2443. [CrossRef]
20. Tao, D.; Luttrell, G.; Yoon, R.-H. A parametric study of froth stability and its effect on column flotation of fine particles. *Int. J. Miner. Process.* **2000**, *59*, 25–43. [CrossRef]
21. Yoon, R.H.; Luttrell, G.H. The effect of bubble size on fine particle flotation. *Miner. Process. Extr. Metall. Rev.* **1989**, *5*, 101–122. [CrossRef]
22. Schubert, H. On the turbulence-controlled microprocesses in flotation machines. *Int. J. Miner. Process.* **1999**, *56*, 257–276. [CrossRef]
23. Schubert, H.; Bischofberger, C. On the microprocesses air dispersion and particle-bubble attachment in flotation machines as well as consequences for the scale-up of macroprocesses. *Int. J. Miner. Process.* **1998**, *52*, 245–259. [CrossRef]
24. Koh, P.; Schwarz, M. CFD modelling of bubble-particle attachments in flotation cells. *Miner. Eng.* **2006**, *19*, 619–626. [CrossRef]